

## Characterization of a gamma-ray source based on a laser-plasma accelerator with applications to radiography

R. D. Edwards, M. A. Sinclair, and T. J. Goldsack

*Hydrodynamics Department, AWE plc, Aldermaston, Reading RG7 4PR, United Kingdom*

K. Krushelnick,<sup>a)</sup> F. N. Beg, E. L. Clark, A. E. Dangor, Z. Najmudin, M. Tatarakis, B. Walton, and M. Zepf

*The Blackett Laboratory, Imperial College of Science, Technology and Medicine, London SW7 2BZ, United Kingdom*

K. W. D. Ledingham and I. Spencer

*Department of Physics and Astronomy, University of Glasgow, Glasgow G12 8QQ, United Kingdom*

P. A. Norreys and R. J. Clarke

*Rutherford Appleton Laboratory, Chilton, Oxon, OX11 0QX, United Kingdom*

R. Kodama, Y. Toyama, and M. Tampo

*Institute of Laser Engineering, Osaka University, 2-6 Yamada-oka, Suita Osaka 565-0871, Japan*

(Received 16 July 2001; accepted for publication 28 January 2002)

The application of high intensity laser-produced gamma rays is discussed with regard to picosecond resolution deep-penetration radiography. The spectrum and angular distribution of these gamma rays is measured using an array of thermoluminescent detectors for both an underdense (gas) target and an overdense (solid) target. It is found that the use of an underdense target in a laser plasma accelerator configuration produces a much more intense and directional source. The peak dose is also increased significantly. Radiography is demonstrated in these experiments and the source size is also estimated. © 2002 American Institute of Physics. [DOI: 10.1063/1.1464221]

High intensity laser-plasma interactions at intensities greater than  $10^{19}$  W/cm<sup>2</sup> have recently allowed the exploration of new regimes in plasma physics. Such interactions can produce fast electrons with energies greater than 100 MeV,<sup>1</sup> x rays of tens of MeV,<sup>2</sup> and energetic ions of up to several hundred MeV.<sup>3</sup> There are clearly many potential applications for these energetic particles such as compact accelerators,<sup>1</sup> inertial fusion,<sup>4</sup> and as diagnostic probe beams of high density material. The use of these lasers as a source of MeV x rays for providing deep-penetration radiographs of dense matter has also recently been discussed.<sup>5</sup> This application of laser-produced plasmas is particularly attractive since such sources may soon be scalable to “tabletop” sizes and to high repetition rates. It may also be possible to obtain multiple views of an object from arbitrary angles—thus potentially enabling three-dimensional radiographic “movies” of dense, rapidly moving objects such as inertially confined fusion targets.

This letter describes experiments conducted at the Rutherford Appleton Laboratory using the ultrahigh power Vulcan laser facility to examine the feasibility of this application. In this work, we compare the use of both high Z solid targets and low density gas jet targets for gamma-ray generation. X rays and gamma rays are generated in a secondary process since electrons are initially accelerated during the laser plasma interaction which subsequently emit hard x rays via bremsstrahlung as they are stopped in solid material. In this work, we show that the x rays produced in a laser accelerator configuration (self-modulated laser Wakefield)<sup>1</sup> are

much more collimated and can be generated more efficiently than in a simple solid target interaction in which the electrons are accelerated by resonance absorption or  $\mathbf{j} \times \mathbf{B}$  ponderomotive acceleration.<sup>2</sup>

In these experiments, we used lithium fluoride thermoluminescent dosimeters (TLDs) to measure the total radiation output as well as the direction and the spectrum of the radiation. The x-ray source was then also used to radiograph thick high-density test objects. The laser interaction region was surrounded by an array of sixteen 5 cm diameter tungsten collimators to provide complete angular information concerning the x-ray flux. The tungsten collimators were constructed using specially made kinematic mounts so that their positions were known precisely. The dosimetry was performed by inserting four standard color-coded plastic containers holding TLD powder which were separated by 4 mm long cylindrical tungsten plugs in a 5 mm diameter 10 cm long cylindrical hole in the center of each of the collimators. These collimators were distributed around the target chamber and the doses on each TLD were measured after single shots. The lithium fluoride 700 powder used in the TLDs was calibrated against a cobalt 60 radioactive source. In addition to the TLD/collimator assemblies which measured filtered dose (behind varying amounts of tungsten), a number of TLDs were fielded to look at the “bare” dose. These were placed inside small Perspex cylinders to ensure electron equilibrium and were sensitive to photon energies above 10 keV.

In these experiments the Vulcan high power beam was transported into an evacuated target chamber where it was focused by an off-axis parabolic mirror to a spot of about 10  $\mu$ m diameter. The pulse length was 0.9–1.2 ps and the total

<sup>a)</sup>Electronic mail: Kmkr@ic.ac.uk

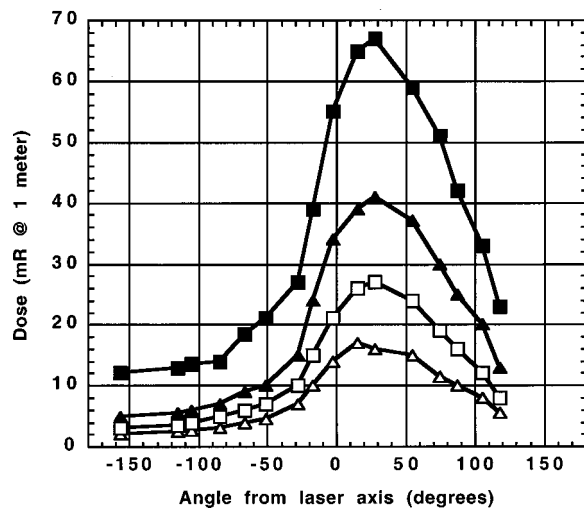


FIG. 1. TLD dose levels with respect to angle for a typical 1 mm tantalum solid target shot with 80 J on target. The peak signal occurs in the direction approximately normal to the target surface ( $45^\circ$ ). (■) first TLD in collimator, 4 mm tungsten filter; (▲) second TLD, 8 mm tungsten filter; (□) 12 mm tungsten filter; (△) 16 mm tungsten filter.

energy was typically 80 J. The maximum intensity was about  $5 \times 10^{19}$  W/cm<sup>2</sup> in the work described here and was estimated by simultaneous measurements of the pulse energy, pulse duration and focal spot size. In the initial set of experiments a solid target was used which was angled at  $45^\circ$  to the direction of beam propagation.

For simplicity the laser generated electron beam was characterized by an “effective” electron temperature ( $T_{\text{effective}}$ ). This is the energy of a monoenergetic electron beam which would produce a similar bremsstrahlung radiation source as produced by the laser. Note that the actual shape of the electron distribution is much more complex and is typically a combination of two exponentials with “hot” and “cold” temperatures. Consequently, the attenuation values for the TLDs through the collimator were calculated for each TLD for varying energies from 0.2 to 14 MeV. The attenuation of gamma rays by the target itself is likely to be small since the targets were less than 2 mm thick. To derive the energy from a particular interaction, ratios from the first TLD to the others in the same collimator were used. The x-ray spectrum could then be deduced by comparing the ratios of the fielded TLDs to predicted values for a given effective energy.

A total of 22 shots were fired with TLDs fielded during this set of experiments and a maximum of 70 TLD containers were used per shot. Background measurements were taken regularly to maintain the accuracy of the TLDs with low readings. Fourteen shots were fired using a solid target of gold or tantalum of differing thicknesses.

Figure 1 shows raw TLD measurements taken from a typical shot onto solid tantalum targets  $-1.75$  mm thick and angled at  $45^\circ$  to the laser axis of propagation. In general, such shots produce their peak dose at an angle of about  $30^\circ$  to the laser beam axis into the target. Unfortunately, TLDs could not be fielded at  $45^\circ$  where the peak dose would have been expected due to space limitations. For each angle three values for  $T_{\text{effective}}$  could be generated, one from each pair of TLD containers within each collimator. An average was then taken to estimate a single  $T_{\text{effective}}$  for the x-ray spectrum.

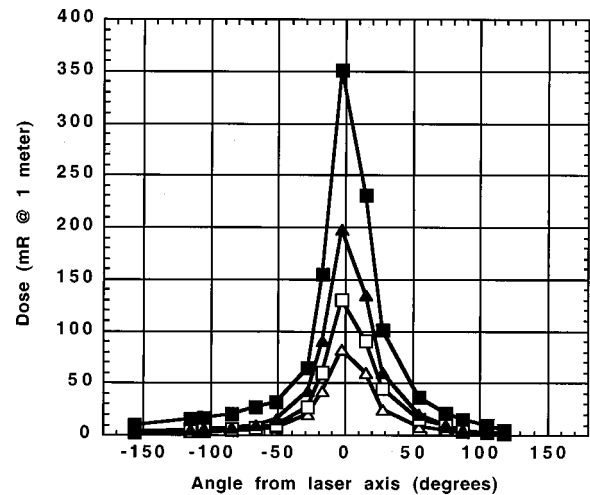


FIG. 2. TLD dose levels with respect to angle for a typical gas jet target shot with 1 mm tantalum bremsstrahlung converter behind. The peak signal occurs in the direction along the direction of laser propagation ( $0^\circ$ ). Vulcan produced 89 J on target.

All of the shots from solid target interactions are broadly similar, with a peak temperature in the direction of the peaks dose of about  $4 \pm 1$  MeV. The main difference between measured angular distributions for different shots are slight changes in the position of the high and low energy points. In all cases, however, the high dose measurements were made on the TLDs facing the back surface of the target, while significantly lower measurements were obtained from the TLDs facing the front, laser illuminated, surface of the target in agreement with previous nuclear activation measurements.<sup>2</sup>

Using the gas target in a laser accelerator configuration as the source of the electron beam has a dramatic effect on the production of x-rays within a high Z target, as shown in Fig. 2. The peak dose is substantially increased over the x rays produced from laser–solid target. In fact, the peak dose may well have been higher than indicated but has been missed by the positioning of the TLDs. The other notable effect is that the width of the dose distribution is considerably narrower and the direction of the x-ray beam (less than  $10^\circ$ ) is directly along the laser axis.

It appears that the high energy electrons which the laser beam generates in the gas jet are well collimated and are highly directional. Evidence for this comes from the shape of the x-ray beam and the difference between the peak doses of these gas jet shots and those without. All of the gas jet shots have a small ( $\sim 5^\circ$ ) mean angle. This implies that the gas jet acts as a source of near unidirectional electrons which then hit the heavy metal target. Rough estimates of the total radiated x-ray dose give similar values to the solid and gas jet shots showing that the change in the on-axis dose is caused by the mean angle of the electron beam created by the laser. This is in contrast to previous activation measurements<sup>6</sup> which showed a much higher signal level relative to solid targets, however, this was likely caused by the fact that activation measurements<sup>7</sup> only record signal from the highest energy x rays while the TLDs record signal from lower energy x rays as well. From the TLD measurements a peak “bare” dose of 2.3 R at 1 m and a  $T_{\text{effective}}$  of  $4.5 \pm 1.5$  MeV was recorded. This is significantly higher than

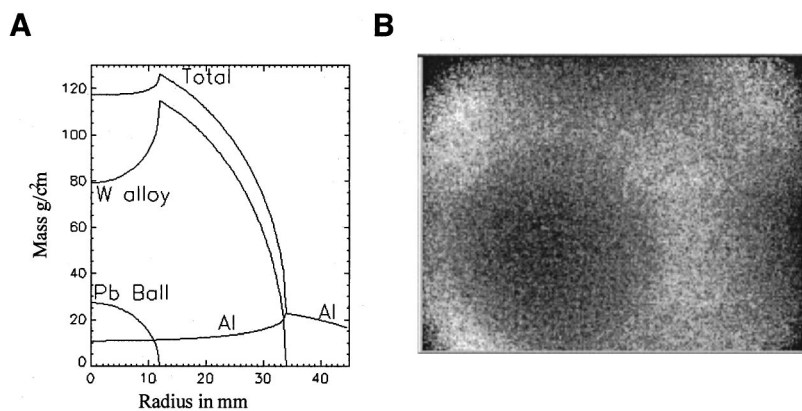


FIG. 3. (A) Line of site mass and (B) radiograph of Vulcan test object produced with a gas jet and 1 mm gold target. Vulcan produced  $\sim 80$  J on target.

previous solid-target measurements performed at much higher laser energy.<sup>5</sup>

Radiography of test objects was also performed using this source. It should be noted that no x-ray collimation or scatter control measures were employed because of space limitations. Had such techniques been used a substantial improvement in the quality of the radiographic images would have been expected. The test object was specifically designed to represent a high-density spherical object. It has an inner sphere of lead, 12 mm in radius, surrounded by a tungsten sphere 35 mm in radius which is itself contained within an aluminum sphere of 53 mm radius. With an incident dose of 156 mR, a density of 0.7 on Kodak DEF direct recording x-ray film would be expected. The actual recorded optical density of the central core had a value of 0.9 (of which 0.2 was inherent background optical density). This is in good agreement with the optical density one would have obtained with an electron beam flash x-ray machine. This was confirmed by radiographing the same object with the Mogul D, x-ray facility at AWE which has a  $T_{\text{effective}}$  (determined using voltage monitors) of 5 MeV and an x-ray source size of 5 mm.

An example radiograph is shown in Fig. 3(B). The source size was estimated to be  $20 \mu\text{m}$ . Shown is the central lead core which has a line of sight mass of  $118 \text{ g/cm}^2$ . The fuzziness to the edge of the lead core is due purely to the lack of collimation and scatter control employed in these proof-of-principle experiments. In the case of the Vulcan laser with the above geometry, blur due to the radiographic source spot diameter of 0.03 mm is 0.0069 mm (spot blur). The intrinsic film blur on DEF film for the Vulcan laser projected into the object plane is 0.284 mm.

In conclusion, we measured the angular direction of x-ray emission from both solid target and gas jet interactions and it appears that the use of a laser accelerator configuration greatly enhanced the collimation and strength of the emitted x-ray beam. Consequently, the use of a well controlled gas-

jet target has clear advantages over solid targets for laser-driven radiography.<sup>8</sup> An important application of these sources may be for nondestructive inspection of rapidly moving materials using high repetition rate lasers. With the ongoing construction of several more powerful laser facilities around the world it seems quite certain that such sources will become extremely useful for radiographic applications.

The authors would like to acknowledge the assistance of the operations staff of the VULCAN Laser at the Rutherford Appleton Laboratory.

<sup>1</sup>A. Modena, Z. Najmudin, A. E. Dangor, C. E. Clayton, K. A. Marsh, C. Joshi, V. Malka, C. B. Darrow, C. Danson, D. Neely, and F. N. Walsh, *Nature (London)* **377**, 606 (1995).

<sup>2</sup>M. H. Key, M. D. Cable, T. E. Cowan, K. G. Estabrook, B. A. Hammel, S. P. Hatchett, E. A. Henry, D. E. Hinkel, J. D. Kilkenny, J. A. Koch, W. L. Krueer, A. B. Langdon, B. F. Lasinski, R. W. Lee, B. J. MacGowan, A. MacKinnon, J. D. Moody, M. J. Moran, A. A. Offenberger, D. M. Pennington, M. D. Perry, T. J. Phillips, T. C. Sangster, M. S. Singh, M. A. Stoyer, M. Tabak, G. L. Tietbohl, M. Tsukamoto, K. Wharton, and S. C. Wilks, *Phys. Plasmas* **5**, 1966 (1998); M. I. K. Santala, E. Clark, I. Watts, F. N. Beg, M. Tatarakis, M. Zepf, K. Krushelnick, A. E. Dangor, T. McCanny, I. Spencer, R. P. Singhal, K. W. D. Ledingham, S. C. Wilks, A. C. Machacek, J. S. Wark, R. Allott, R. J. Clarke, and P. A. Norreys, *Phys. Rev. Lett.* **84**, 1459 (2000).

<sup>3</sup>E. L. Clark, K. Krushelnick, M. Zepf, F. N. Beg, M. Tatarakis, A. Machacek, M. I. K. Santala, I. Watts, P. A. Norreys, and A. E. Dangor, *Phys. Rev. Lett.* **85**, 1654 (2000).

<sup>4</sup>M. Tabak, J. Hammer, M. E. Glinsky, W. L. Krueer, S. C. Wilks, J. Woodworth, E. M. Campbell, M. D. Perry, and R. J. Mason, *Phys. Plasmas* **1**, 1626 (1994).

<sup>5</sup>M. D. Perry, J. A. Sefcik, T. Cowan, S. Hatchett, A. Hunt, M. Moran, D. Pennington, R. Snavely, and S. C. Wilks, *Rev. Sci. Instrum.* **70**, 265 (1999).

<sup>6</sup>M. I. K. Santala, Z. Najmudin, E. L. Clark, M. Tatarakis, K. Krushelnick, A. E. Dangor, V. Malka, J. Faure, R. Allott, and R. J. Clarke, *Phys. Rev. Lett.* **86**, 1227 (2001).

<sup>7</sup>W. P. Leemans, D. Rodgers, P. E. Catravas, C. G. R. Geddes, G. Fubiani, E. Esarey, B. A. Shadwick, R. Donahue, and A. Smith, *Phys. Plasmas* **8**, 2510 (2001).

<sup>8</sup>O. L. Landen, D. R. Farley, S. G. Glendinning, L. M. Logory, P. M. Bell, J. A. Koch, F. D. Lee, D. K. Bradley, D. H. Kalantar, C. A. Back, and R. E. Turner, *Rev. Sci. Instrum.* **72**, 627 (2001).